LHCb Collaboration

LHCb 2002-034
17 March 2002

Construction and Test of the Prototype Chamber for Region 1 of the LHCb Muon Station 2

Bernard Maréchal, Gisele de Oliveira, Leandro de Paula, Miriam Gandelman
LAPE - Instituto de Física, Universidade Federal do Rio de Janeiro, Rio de Janeiro, Brazil
Hector Costa, Roberto da Silva
CEFET-RJ, Rio de Janeiro, Brazil
Anatoli Kashchuk, Thomas Schneider
European Laboratory for Particle Physics (CERN), Geneva, Switzerland

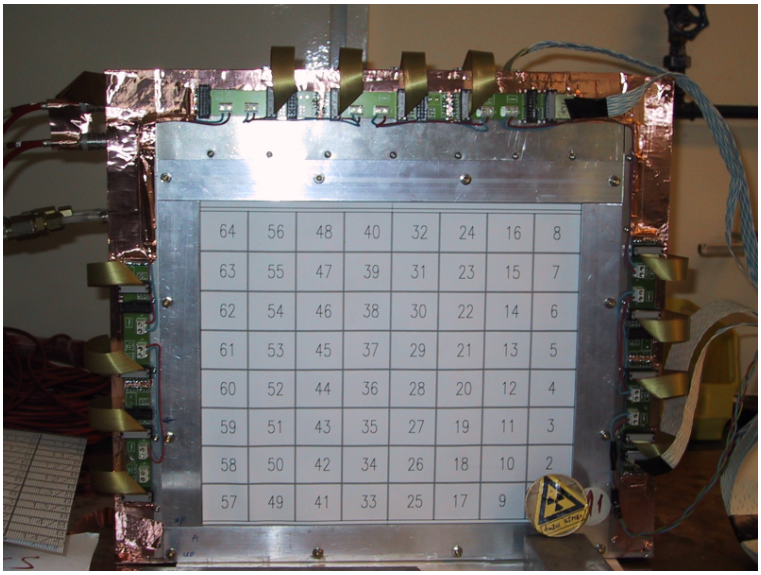

Abstract

A four gap MWPC prototype for region 1 of the muon station 2, with non-staggered wires, was built and tested. The construction details and the test results are presented.

1 Introduction

The LHCb muon system [1] will use Multi-Wire Proportional Chambers (MWPC) for the four regions of stations 2 and 3, for regions 3 and 4 of station 1 and for regions 1 and 2 of stations 4 and 5. The chambers vary in size for the different stations and regions and they have different readout pad sizes in those regions (see [2] for more details). In this note, the construction of a MWPC prototype for region 1 of station 2 is described. The prototype is an exact realization of a chamber for this region. It has four symmetric gas gaps and the characteristics listed in table 1.

Table 1: Some chamber parameters and operation conditions.

Gas Gap size (mm)	5
Anode-Cathode spacing (mm)	2.5
Wire Diameter (μm)	30
Sensitive area (mm^2)	300$\times$250
Wire pitch (mm)	1.5
Wire pad size (mm^2)	6.3$\times$250
Wire length (mm)	257
Cathode pad size (mm^2)	37.5$\times$31.3
Wire Tension (gf)	60 ± 10
Nominal Gas mixture	$\mathrm{Ar/CO_2/CF_4}$ (40% 50% 10%)
Wire nominal potential (V)	3150

The chamber has a combined readout of wire and cathode pads as a consequence of the required granularity.

2 Chamber Construction

The prototype was built in Rio (CEFET-RJ and LAPE/IF-UFRJ) with PCB-honeycomb-PCB panels as described in the Muon System TDR [1]. The panels' flatness was measured (INMETRO[1] and Bargoa[2]) to be within $\pm 40\mu$m, which is better than the required specifications (see [3]). The wire fixation bars were also measured and glued to the cathode panels. The anode to cathode distance was insured by means of a precise steel spacer fixed to those bars, during the gluing of the wires. For the present prototype the wire fixation bars were not machined to have a *nose* on the edges which was done for the previous prototypes to avoid discharges [3]. The results for the dark current and the spark limit show that this *nose* is not necessary. The dark current measured was of the order of the nA and the spark limit was of about 3.45 kV.

The wiring was done in a lathe as shown in the picture of figure 1. The wire tension was guaranteed using a calibrated device as shown in figure 2. This device has a DC motor that keeps the wire under tension by applying a torque on the reel. The DC voltage applied to the motor was calibrated with a 60 gf weight.

[1]Instituto Nacional de Metrologia, Normalização e Qualidade Industrial, Rio de Janeiro

[2]Bargoa Conectores, Rio de Janeiro

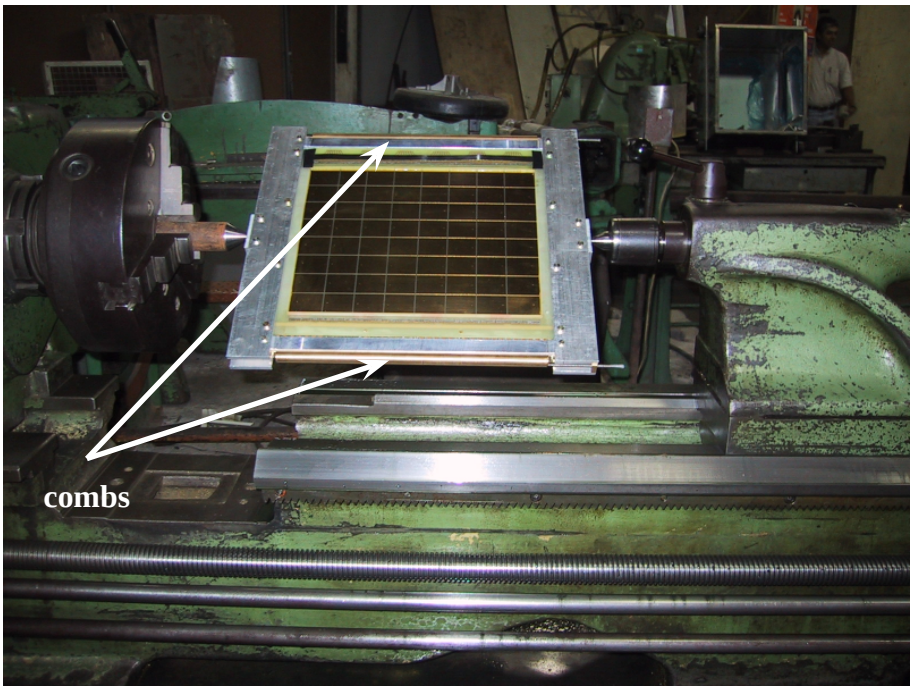

Figure 1: One of the cathode planes mounted to the frame to be wired in the lathe.

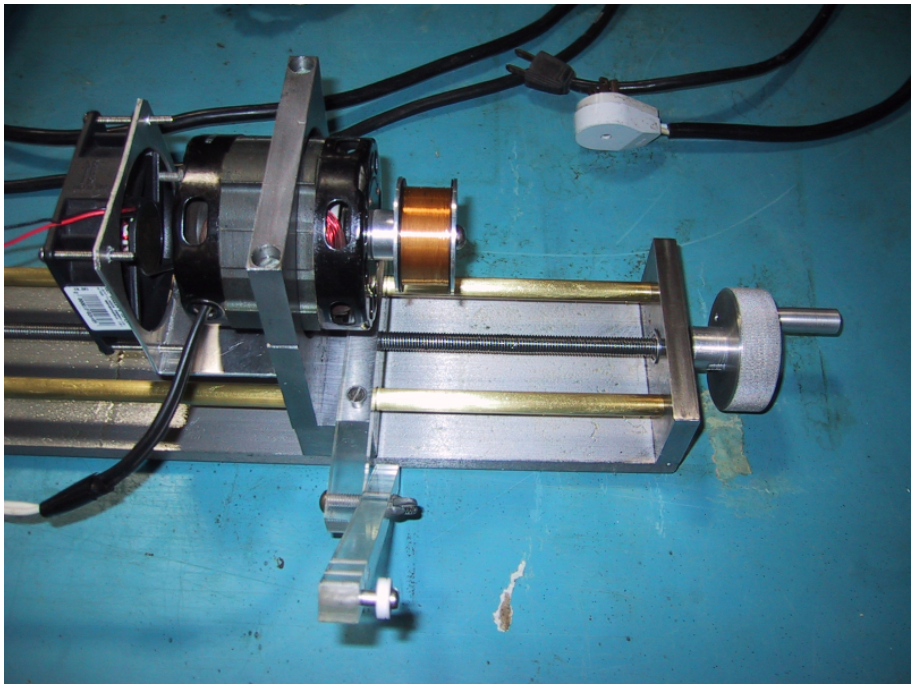

Figure 2: The device used to garantee the wire tension. A DC motor is mounted on an endless screw used to advance the wire reel.

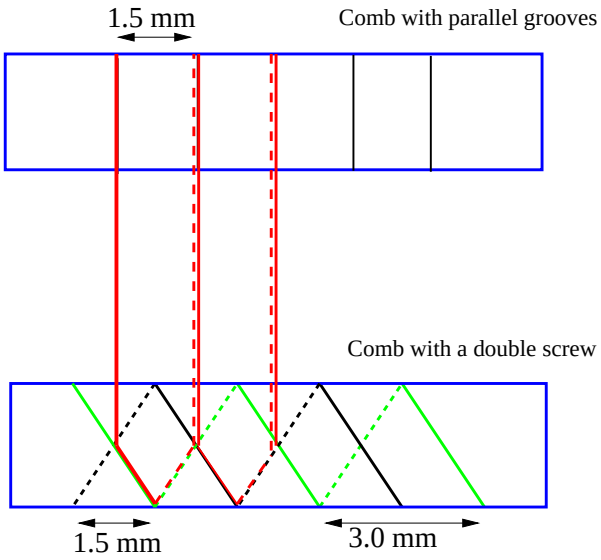

Figure 3: Schematic drawing of the non-staggered wiring scheme. The two different combs are shown.

Since the wire pad size is very small (6.3 mm, 4 wires only), it was required that the anode planes had non-staggered wires to minimize cross-talk effects. The wiring was done with combs directly around the cathode planes. Due to that, the combs had to be designed as shown in figure 3. The two combs are different from each other, one having a double screw and the other, just parallel grooves. Figure 1 shows the combs mounted onto the frame around the cathode plane on the lathe. After wiring the wire pitch was measured to be (1.501 ± 0.018) mm, which satisfies the required precision.

The wires were then glued and soldered to the wire fixation bars. Having the five panels ready (two with the four wire planes, the two outer ground planes and the middle ground plane), the chamber was mounted as can be seen in the pictures of figure 4. On the right picture one can see the mounting of the planes and on the left, the chamber ready to have the electronics mounted to it.

3 Test Results

3.1 Front-End Electronics

The chamber anode and cathode combined readout is shown in figure 5. The front-end scheme is the same of the previous prototypes using the ASDQ++ [4] as the front-end chip. Each front-end board was equipped with two ASDQ++ chips, each reading 8 channels. The threshold voltage was set to 400mV (10fC) for the anode and 250mV (5fC) for the cathode readout, since for the latter the signal is shared between the two cathode planes.

The chamber was fully equipped with the front-end electronics but only 32 channels could be readout at a time due to the data acquisition limited number of TDC channels. Figure 5 also shows a schematic view of the chamber with the 8 cathode and 8 anode pads of one double gap readout by the data acquisition system. The other 16 channels belongs to the second double gap. The 8 wire pads cover a 50×250 mm^2 area and the 8 cathode pads, a 150×62 mm^2 area.

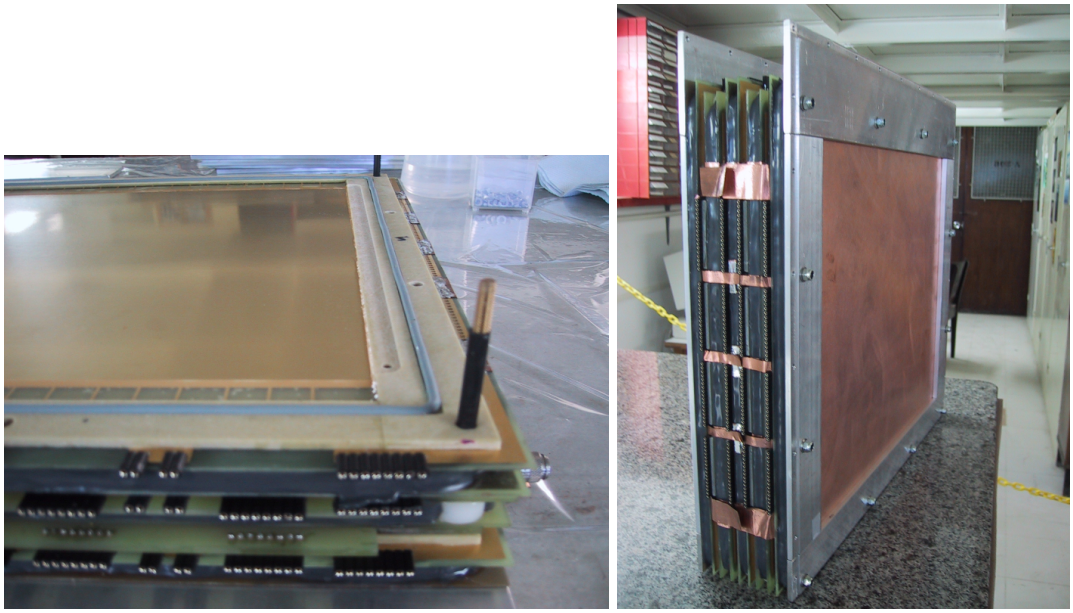

Figure 4: Left: the final mounting of the chamber panels. Right: The chamber ready to have the electronics mounted to it.

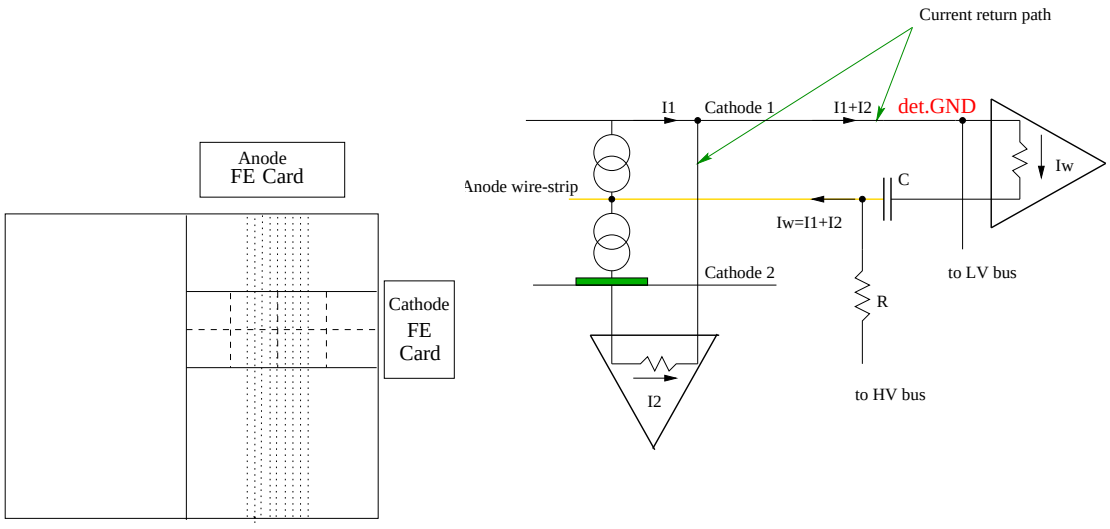

Figure 5: Left: Schematic drawing of the chamber anode and cathode pads readout. Right: Combined readout scheme.

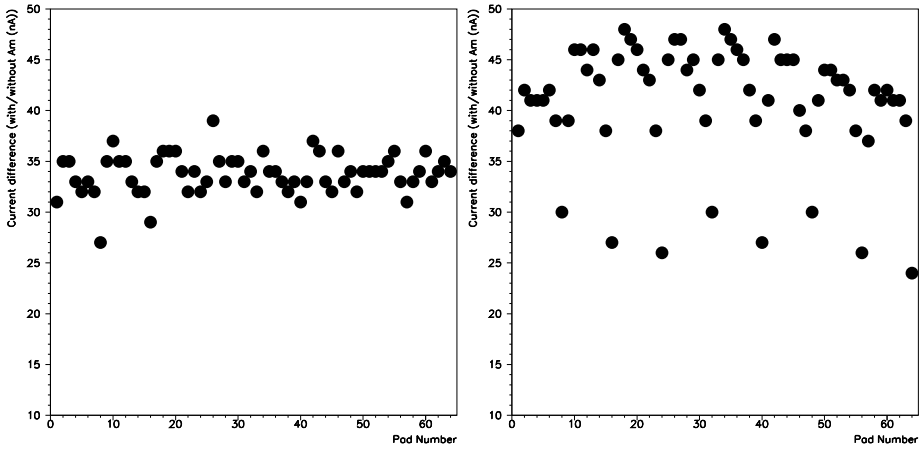

Figure 6: Current measured with the americium source (zero subtracted) versus the pad number for double gaps A (left) and B (right). The applied high voltage was 3.0kV. The eight lower points in the plot for the double gap B correspond to one row of pads on the border of the chamber (row of pads numbers 8 to 64 seen on the picture on the cover page).

3.2 ^{241}Am Test Results

After two days of training (positive high voltage during the day and negative during the night), the detector was tested with an americium source to see the current uniformity in all detector pads. The results show a good uniformity for one of the double gaps (called double gap A) and a row of lower current pads on the second double gap (double gap B). Those results are presented in the plots of figure 6. The effect seen for the double gap B is true for both single gaps B1 and B2 which have a row of pads with lower current and also a banana shaped distribution. This might indicate a mechanical deformation or gap bars with slightly different widths.

3.3 Beam Test Results

The beam tests were performed in the T11 beam area with the main goal to investigate the cluster size in four-gap chambers with small pad sizes and irradiated by particle tracks not perpendicular to the wire planes. Indeed at region 1 of this station, tracks coming from the interaction point of up to 3^o degrees could cross the chambers. Since the chamber has four gaps and a distance of about 4.5 cm from the first to the last wire plane, a track passing one pad in the first gap has around 30% probability to arrive on a neighboring pad at the last gap. The total cluster size is due to this effect and to the fact that a track may cross the anode plane between two pads. Since this prototype has four wires per pad the latter effect can be significant.

A schematic view of the T11 setup is shown in Figure 7. There one can see the two counters (S1 and S2) used in coincidence for the trigger. S1 is a 20×20 cm^2 scintillator and S2 is 15×15 cm^2. Also shown is the X-Y hodoscope used for the off-line selection. The hodoscope has 8 vertical and 8 horizontal scintillators, each of 8×1 cm^2, forming a grid of 64 1×1 cm^2 cells. Only events passing simultaneously one vertical and one horizontal channel were considered in the analysis. The 4-gap chamber was positioned between the S1 counter and the hodoscope.

A beam of 3 GeV protons and pions with rates varying from 8 kHz to 150 kHz (as seen from the S1 counter) was used. Figure 8 shows a typical beam profile as seen by the hodoscope (left). The middle and rightmost plots show the cathode and anode channels fired when there

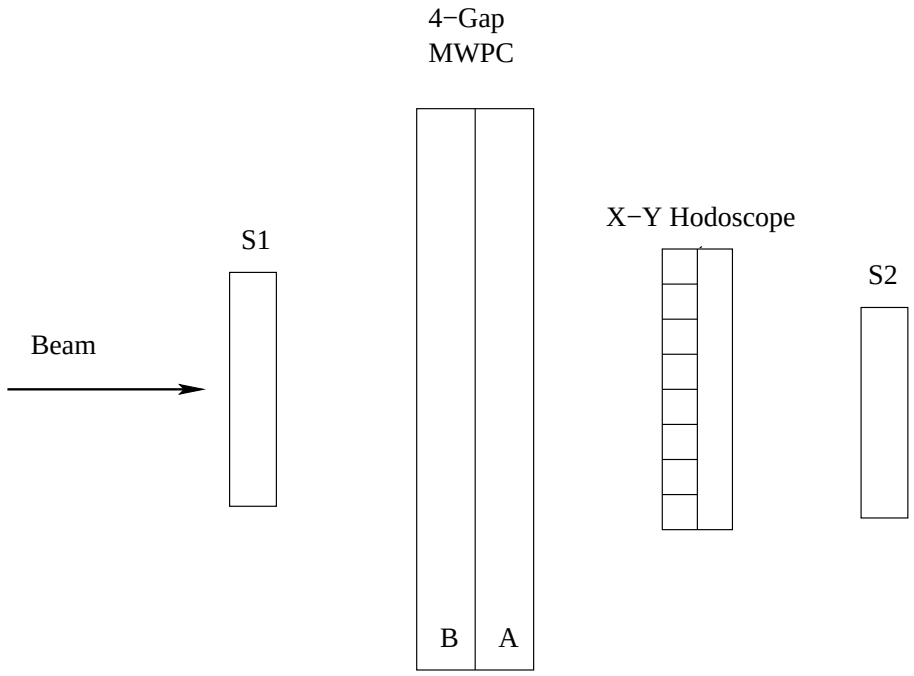

Figure 7: The beam test experimental setup in the T11 area.

is a hit in the most populated cell of the hodoscope. Due to the hodoscope cell size, more than one anode channel is selected in this way.

3.3.1 Efficiency

The efficiency plateaus presented here were obtained for a 20ns time window for each individual double gap and for the OR of the four gaps. Figure 9 shows the plateau curves for the nominal gas mixture ($Ar/CO_2/CF_4$ (40% 50% 10%)) for the double gaps A and B as indicated in the figure (top) and the OR of the four gaps for the same gas mixture (bottom). Due to electronics instabilities during some of the runs, the particle flux had to be reduced above 3.25 kV. One can see in the figure that, for the individual double gaps, the anode pads reach 95% efficiency at 3.00 kV but for cathode that happens only around 3.10 kV. This has to be further investigated but could be due to the electronics threshold that maybe too high on the cathode for the 3 GeV particles of the T11 beam area or for the signals from the borders of the pads. The threshold was lowered by 30mV for some runs and the difference in the rising of the plateau was somewhat reduced. Unfortunatelly, due to noise and pick-up problems in the front-end boards, the threshold could not be further reduced. For the OR of the four gaps, the chamber reaches 99.99% for the cathode and for the anode at the nominal voltage (3.15 kV).

Gas leaks were observed, as in all the prototypes built so far. However, these leaks don't seem to affect the performance of the chamber, since after about 12 hours without gas bubbling, the efficiency curves obtained were quite similar to the ones shown here.

Figure 10 shows the same plots for the new gas mixture ($Ar/CO_2/CF_4$ (40% 40% 20%)) where one can see that the plateau becomes slightly wider.

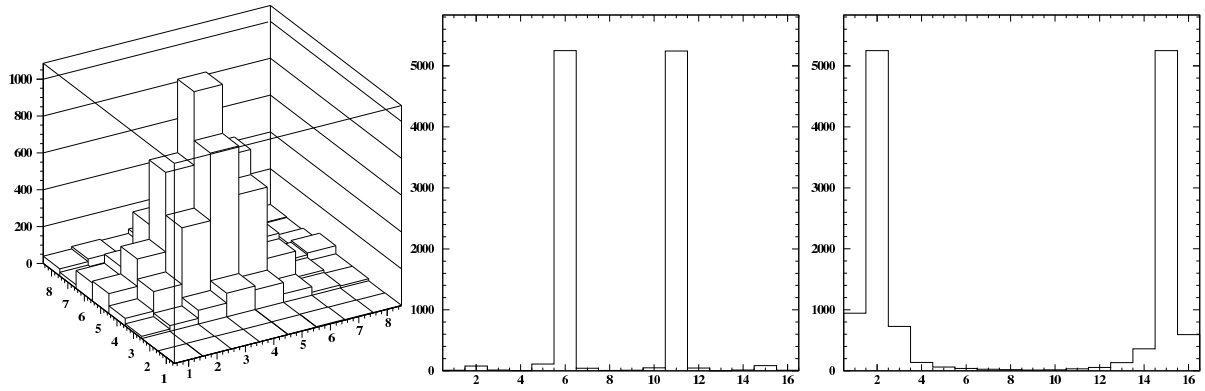

Figure 8: The beam profile in the hodoscope (left) showing that the beam is mostly in the vertical channel 5 and horizontal channel 4 of it. The two peaks in the cathode profile (middle), show that the beam is on channel 6 of one double gap which corresponds to channel 11 in the other gap. For the anode (right), the same holds for channels 2 and 15.

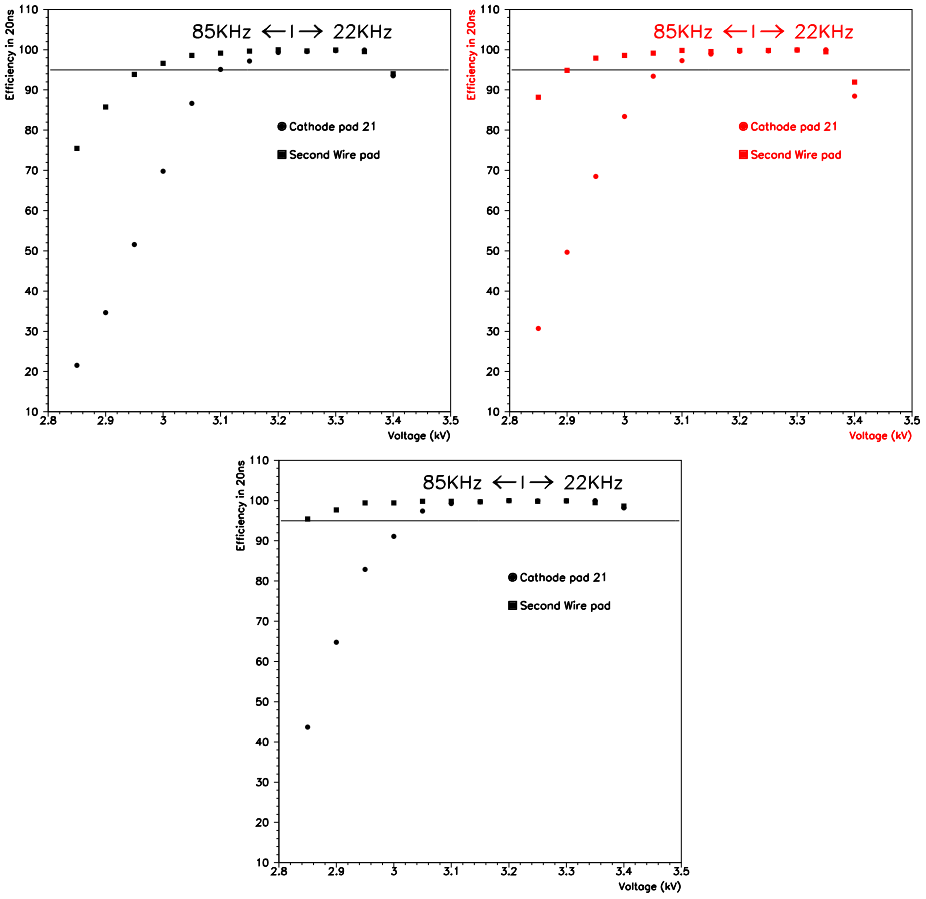

Figure 9: Efficiency plot for the nominal gas mixture (see text). The top plot shows plateau curves for the double gaps A (left) and B and the bottom plot the efficiency for the OR of the four gaps.

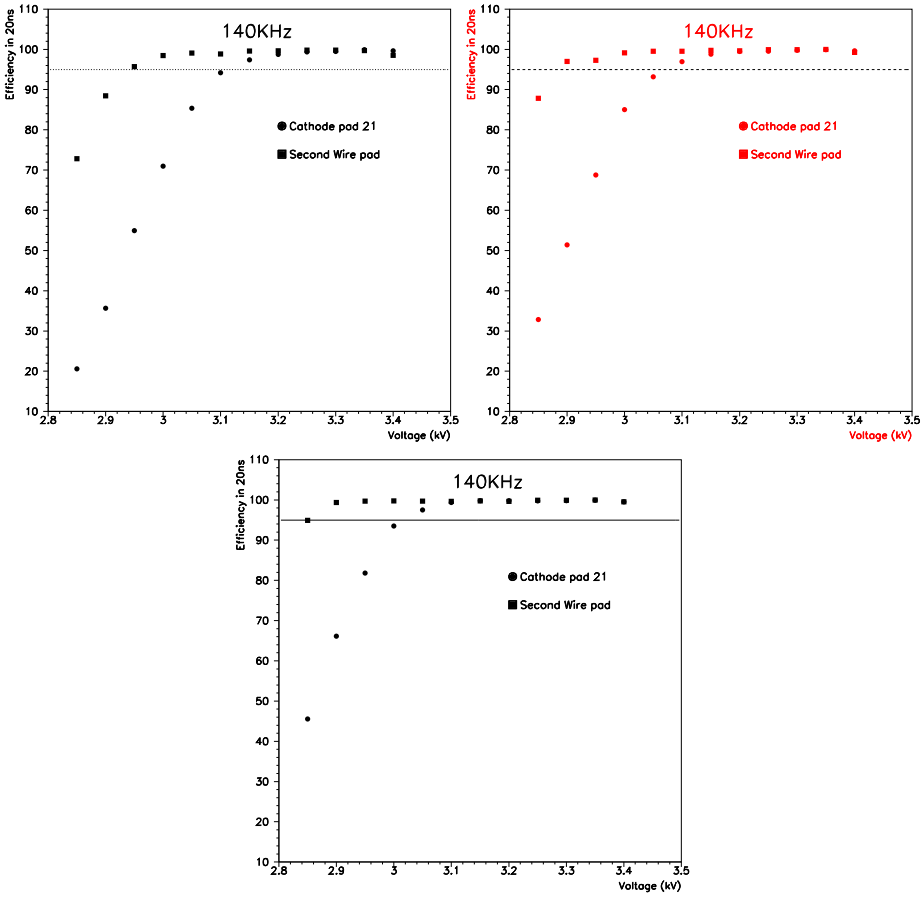

Figure 10: Efficiency plot for the new gas mixture (see text). The top plot shows plateau curves for the double gaps A and B and the bottom plot the efficiency for the OR of the four gaps.

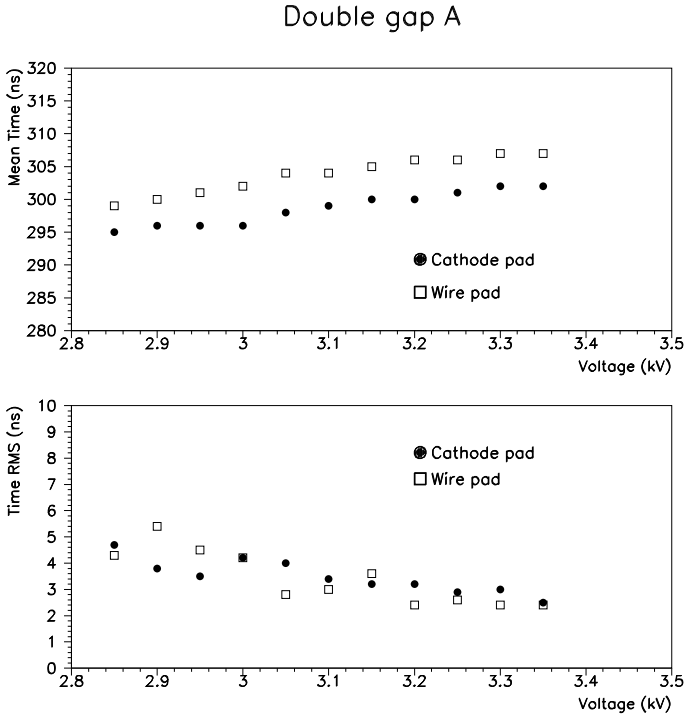

Figure 11: Time walk and resolution as a function of the high voltage for double gap A. The double gap B gives the same results.

3.3.2 Time Resolution and Time Walk

The time walk and resolution are plotted in figure 11 as a function of the high voltage. The results are as expected for the two gas mixture and are the same as for the last prototype tested [5].

3.3.3 Cluster Size

The cluster size is defined as the mean number of fired pads per event selected by having one single hit on the vertical and horizontal hodoscope strips. The typical anode time distribution is shown in figure 12 where one can see two peaks. The smaller peak is due to the discrimination of big enough ASDQ++ pulse undershoots. For the cluster size calculations only the particles arriving first were considered. To do that, a 20 ns time window from 292ns to 312ns was applied to select the in-time hits. The results obtained with the chamber at three different angles with respect to the beam line are shown in figures 13 and 14. On the first figure the results were calculated for one double gap only (double gap A) and on the second, for the OR of the four gaps. In this case, as expected, the geometrical effect of non perpendicular particles crossing the chamber is more visible for the wire pads.

The increasing of the cluster size values as a function of the high voltage can be seen in a scatter plot of the number of fired pads in the cathode versus the same number for the anode of one double gap. In figure 15 one can see this scatter plot for three different voltages. In the rightmost plot a bigger number of events where 8 wire pads have fired can be seen. This means that all the readout channels have fired which should not be the case when a particle crosses the detector and indicates that there might have been some sparks or detector instabilities (electronically induced pulses) at this voltage.

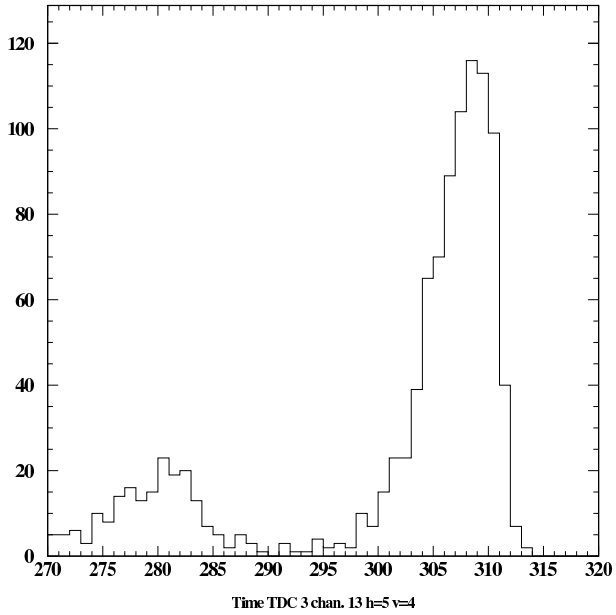

Figure 12: Typical anode time distribution (see text). Due to common stop mode operation of the TDCs, the time increases towards the left. One TDC channel corresponds to 1 ns.

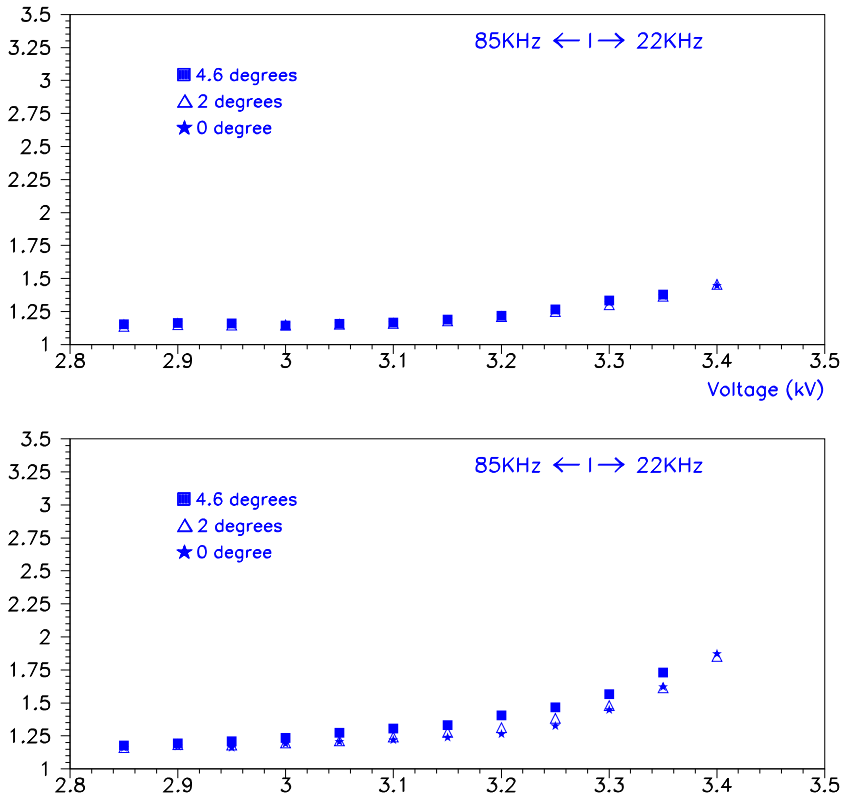

Figure 13: The cluster size values as a function of the high voltage for the double gap A. The top plot shows the results for the cathode, while the bottom, for the anode.

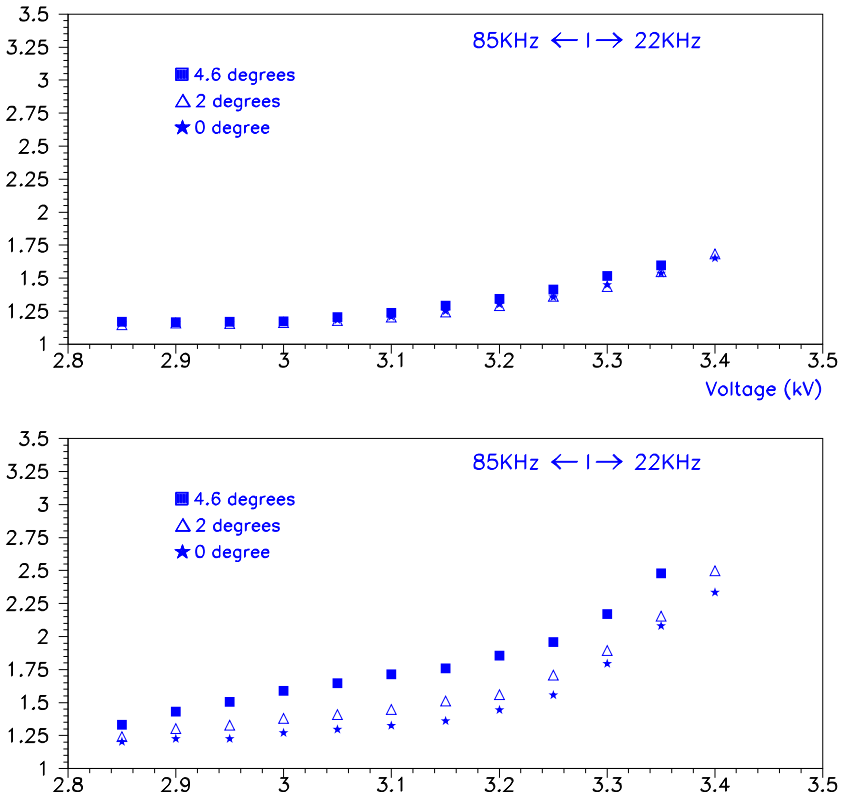

Figure 14: The cluster size values as a function of the high voltage for the OR of the four gaps. The top plot shows the results for the cathode, while the bottom, for the anode.

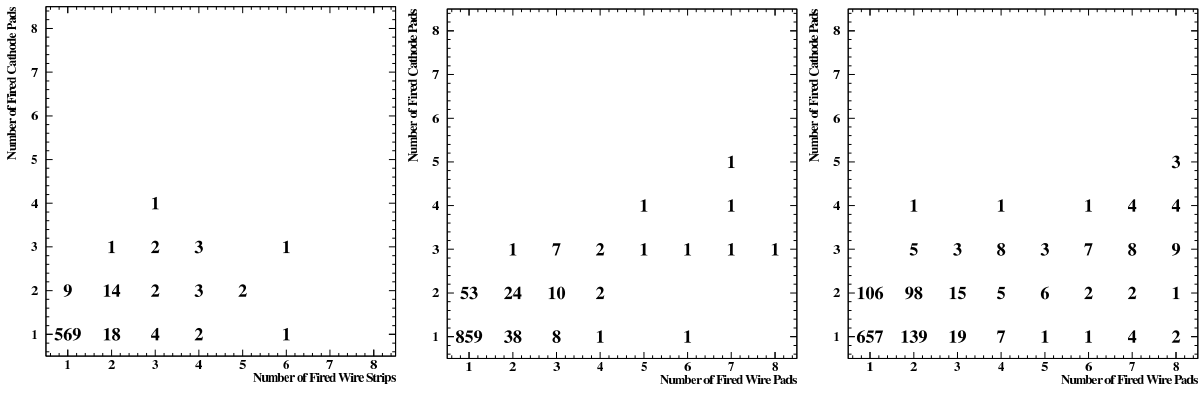

Figure 15: Number of fired cathode pads versus the number of fired wire pads for three different voltages: 3.00kV (left), 3.15kV (middle) and 3.35kV (right).

4 Conclusions

A MWPC prototype for the region 1 of muon station 2 was built and tested in the T11 beam area. The main goal of these tests was to measure the detector cluster size when the chamber four gaps are OR-ed. For the nominal high voltage and gas mixture the cluster size for normal incidence is 1.25 for the cathode and 1.36 for the anode. The achieved efficiency for the nominal voltage is 98.0% for the cathode and 99.6% the anode for the double gaps individually. A difference in the rising of the efficiency plateau was observed, the cathode achieving 95% efficiency 150 V later than the anode. The reason for this should be further investigated, but could be due to the electronics threshold that was too high for the 3 GeV particles of the beam or for the signals from the borders of the pads. For the OR of the four gaps, the chamber reaches 99.99% for the cathode and for the anode at the nominal voltage. No big difference was seen in the detector performance with the new gas mixture ($\mathrm{Ar}/\mathrm{CO_2}/\mathrm{CF_4}$ (40% 40% 20%)).

The detector should now be tested in the X7 beam area together with the previous prototype for comparison. The tests should be done with a better grounding and shielding scheme, using the CARIOCA chip and having at least three times more readout channels if compared to the test done in the T11 area to check the chamber homogeneity.

Before building new prototypes the design and quality control methods should be reviewed to avoid gas leaks and possible mechanical deformations.

5 Acknowledgments

The authors would like to thank B. Schmidt and W. Riegler for the help during the beam test, F. Bediaga and S. da Silva from Bargoa and M. Motta from INMETRO for the metrological measurements, R. B. Monteiro Neto and C. de Alencar from SENAI and A. L. S. Pontes from CAPC-Peças Mecânicas e Industriais Ltda. for the machining of the mechanical pieces.

This work was partially supported by CNPq, FUJB, FAPERJ and the European Commission (contract CT1-CT94-0118).

References

[1] *LHCb Muon System Technical Design Report*, CERN/LHCC 2001-010 LHCb TDR 4, The LHCb Collaboration.

[2] *LHCb muon system by numbers*, LHCb 2000-089 MUON, B. Schmidt.

[3] *Design and Construction of the Wire Chambers for the LHCb Muon System*, LHCb 2001-026 MUON, Kashchuk, A; Kristic, R; Riegler, W; Schmidt, B; Schneider, T; Suvorov, V; Anelli, M; Campana, P; Denni, U; Felici, G; Frani, M. A; Saputi, A; Marechal, B; Gandelman, M; de Paula, L; Carassiti, V; Evangelisti, F; Savrie, M; Botchine, B; Guets, S; Lazarev, V; Vorobyov, A; Auriemma, G; Fidanza, D; Satriano, C.

[4] *Performance study of a MWPC prototype for the LHCb muon system with the ASDQ chip*, LHCb 2000-62, MUON, A. Kashchuk, L. de Paula, W. Riegler, B. Schmidt, T. Schneider.

[5] *Results obtained with the first four gap MWPC prototype chamber*, LHCb-2001-024, MUON, D. Hutchcroft, A. Kachtchouk, W. Riegler, B. Schmidt, T. Schneider, V. Suvorov, B. Marechal, M. Gandelman.